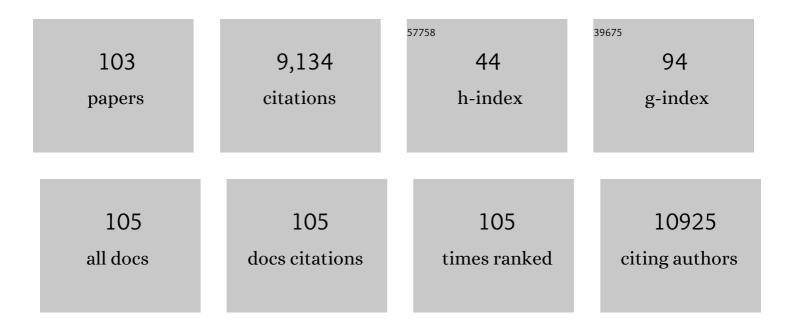
## Donghoe Kim

List of Publications by Year in descending order

Source: https://exaly.com/author-pdf/1873116/publications.pdf Version: 2024-02-01



#	Article	IF	CITATIONS
1	Defect Healing in FAPb(I <sub>1â€</sub> <i><sub>x</sub></i> Br <i><sub>x</sub></i> ) <sub>3</sub> Perovskites: Multifunctional Fluorinated Sulfonate Surfactant Anchoring Enables >21%ÂModules with Improved Operation Stability. Advanced Energy Materials, 2022, 12, .	19.5	32
2	Perovskite microcells fabricated using swelling-induced crack propagation for colored solar windows. Nature Communications, 2022, 13, 1946.	12.8	18
3	Defect Healing in FAPb(I <sub>1â€</sub> <i><sub>x</sub></i> Br <i><sub>x</sub></i> ) <sub>3</sub> Perovskites: Multifunctional Fluorinated Sulfonate Surfactant Anchoring Enables >21%ÂModules with Improved Operation Stability (Adv. Energy Mater. 20/2022). Advanced Energy Materials, 2022, 12, .	19.5	0
4	In situ formation of <scp>Imidazoleâ€Based 2D</scp> interlayer for efficient perovskite solar cells and modules. International Journal of Energy Research, 2022, 46, 15419-15427.	4.5	3
5	High Efficiency Perovskite Solar Cells Exceeding 22% via a Photoâ€Assisted Twoâ€6tep Sequential Deposition. Advanced Functional Materials, 2021, 31, 2006718.	14.9	33
6	Wide-Bandgap Metal Halide Perovskites for Tandem Solar Cells. ACS Energy Letters, 2021, 6, 232-248.	17.4	89
7	Formamidine disulfide oxidant as a localised electron scavenger for >20% perovskite solar cell modules. Energy and Environmental Science, 2021, 14, 4903-4914.	30.8	63
8	Rationally Designed Window Layers for High Efficiency Perovskite/Si Tandem Solar Cells. Advanced Optical Materials, 2021, 9, 2100788.	7.3	7
9	Synthesis and adsorption properties of gelatin-conjugated hematite (α-Fe2O3) nanoparticles for lead removal from wastewater. Journal of Hazardous Materials, 2021, 416, 125696.	12.4	38
10	Intermediate Phaseâ€Free Process for Methylammonium Lead Iodide Thin Film for Highâ€Efficiency Perovskite Solar Cells. Advanced Science, 2021, 8, e2102492.	11.2	20
11	All-in-One Lewis Base for Enhanced Precursor and Device Stability in Highly Efficient Perovskite Solar Cells. ACS Energy Letters, 2021, 6, 3425-3434.	17.4	41
12	Room-Temperature-Processed Amorphous Sn-In-O Electron Transport Layer for Perovskite Solar Cells. Materials, 2020, 13, 32.	2.9	7
13	Largeâ€Scale Assembly of Peptideâ€Based Hierarchical Nanostructures and Their Antiferroelectric Properties. Small, 2020, 16, e2003986.	10.0	6
14	Sustainable lead management in halide perovskite solar cells. Nature Sustainability, 2020, 3, 1044-1051.	23.7	87
15	Enhanced ferroelectric photovoltaic effect in semiconducting single-wall carbon nanotube/BiFeO <sub>3</sub> heterostructures enabled by wide-range light absorption and efficient charge separation. Journal of Materials Chemistry A, 2020, 8, 10377-10385.	10.3	10
16	Enhancing Charge Transport of 2D Perovskite Passivation Agent for Wideâ€Bandgap Perovskite Solar Cells Beyond 21%. Solar Rrl, 2020, 4, 2070065.	5.8	2
17	Tailored 2D/3D Halide Perovskite Heterointerface for Substantially Enhanced Endurance in Conducting Bridge Resistive Switching Memory. ACS Applied Materials & Interfaces, 2020, 12, 17039-17045.	8.0	55
18	Enhancing Charge Transport of 2D Perovskite Passivation Agent for Wideâ€Bandgap Perovskite Solar Cells Bevond 21%, Solar Rrl, 2020, 4, 2000082.	5.8	79

#	Article	IF	CITATIONS
19	Efficient, stable silicon tandem cells enabled by anion-engineered wide-bandgap perovskites. Science, 2020, 368, 155-160.	12.6	420
20	Revisiting Effects of Ligand-Capped Nanocrystals in Perovskite Solar Cells. ACS Energy Letters, 2020, 5, 1032-1034.	17.4	19
21	Unassisted Water Splitting Exceeding 9% Solar-to-Hydrogen Conversion Efficiency by Cu(In, Ga)(S, Se)2 Photocathode with Modified Surface Band Structure and Halide Perovskite Solar Cell. ACS Applied Energy Materials, 2020, 3, 2296-2303.	5.1	31
22	26.7% Efficient 4-Terminal Perovskite–Silicon Tandem Solar Cell Composed of a High-Performance Semitransparent Perovskite Cell and a Doped Poly-Si/SiOx Passivating Contact Silicon Cell. IEEE Journal of Photovoltaics, 2020, 10, 417-422.	2.5	40
23	Real Impacts of Ligand-Capped Nanocrystals in Perovskite Solar Cells. ECS Meeting Abstracts, 2020, MA2020-02, 1901-1901.	0.0	0
24	Ultimate Charge Extraction of Monolayer PbS Quantum Dot for Observation of Multiple Exciton Generation. ChemPhysChem, 2019, 20, 2657-2661.	2.1	1
25	Bimolecular Additives Improve Wide-Band-Gap Perovskites for Efficient Tandem Solar Cells with CIGS. Joule, 2019, 3, 1734-1745.	24.0	227
26	Ternary diagrams of the phase, optical bandgap energy and photoluminescence of mixed-halide perovskites. Acta Materialia, 2019, 181, 460-469.	7.9	14
27	Carrier lifetimes of >1 μs in Sn-Pb perovskites enable efficient all-perovskite tandem solar cells. Science, 2019, 364, 475-479.	12.6	781
28	Enhanced Charge Transport in 2D Perovskites via Fluorination of Organic Cation. Journal of the American Chemical Society, 2019, 141, 5972-5979.	13.7	274
29	Insights into operational stability and processing of halide perovskite active layers. Energy and Environmental Science, 2019, 12, 1341-1348.	30.8	125
30	Effect of TiO2 particle size and layer thickness on mesoscopic perovskite solar cells. Applied Surface Science, 2019, 477, 131-136.	6.1	57
31	Organic-Inorganic Perovskite for Highly Efficient Tandem Solar Cells. Ceramist, 2019, 22, 146-169.	0.1	1
32	Highly Efficient Perovskite Solar Modules by Scalable Fabrication and Interconnection Optimization. ACS Energy Letters, 2018, 3, 322-328.	17.4	143
33	Scalable Deposition of High-Efficiency Perovskite Solar Cells by Spray-Coating. ACS Applied Energy Materials, 2018, 1, 1853-1857.	5.1	78
34	Boosting the solar water oxidation performance of a BiVO <sub>4</sub> photoanode by crystallographic orientation control. Energy and Environmental Science, 2018, 11, 1299-1306.	30.8	330
35	Scalable fabrication of perovskite solar cells. Nature Reviews Materials, 2018, 3, .	48.7	764
36	Effect of non-stoichiometric solution chemistry on improving the performance of wide-bandgap perovskite solar cells. Materials Today Energy, 2018, 7, 232-238.	4.7	31

#	Article	IF	CITATIONS
37	Scalable Deposition of Polycrystalline Perovskite Thin Films towards High-Efficiency and Large-Area Perovskite Photovoltaics. , 2018, , .		0
38	3D/2D multidimensional perovskites: Balance of high performance and stability for perovskite solar cells. Current Opinion in Electrochemistry, 2018, 11, 105-113.	4.8	59
39	Simultaneous Ligand Exchange Fabrication of Flexible Perovskite Solar Cells using Newly Synthesized Uniform Tin Oxide Quantum Dots. Journal of Physical Chemistry Letters, 2018, 9, 5460-5467.	4.6	31
40	Stable Formamidiniumâ€Based Perovskite Solar Cells via In Situ Grain Encapsulation. Advanced Energy Materials, 2018, 8, 1800232.	19.5	78
41	Perovskite Solar Cells: Stable Formamidinium-Based Perovskite Solar Cells via In Situ Grain Encapsulation (Adv. Energy Mater. 22/2018). Advanced Energy Materials, 2018, 8, 1870101.	19.5	1
42	Scalable slot-die coating of high performance perovskite solar cells. Sustainable Energy and Fuels, 2018, 2, 2442-2449.	4.9	155
43	Outlook and Challenges of Perovskite Solar Cells toward Terawatt-Scale Photovoltaic Module Technology. Joule, 2018, 2, 1437-1451.	24.0	162
44	Do grain boundaries dominate non-radiative recombination in CH <sub>3</sub> NH <sub>3</sub> PbI <sub>3</sub> perovskite thin films?. Physical Chemistry Chemical Physics, 2017, 19, 5043-5050.	2.8	161
45	Extrinsic ion migration in perovskite solar cells. Energy and Environmental Science, 2017, 10, 1234-1242.	30.8	458
46	300% Enhancement of Carrier Mobility in Uniaxialâ€Oriented Perovskite Films Formed by Topotacticâ€Oriented Attachment. Advanced Materials, 2017, 29, 1606831.	21.0	120
47	Highly Efficient and Uniform 1 cm <sup>2</sup> Perovskite Solar Cells with an Electrochemically Deposited NiO <sub><i>x</i></sub> Holeâ€Extraction Layer. ChemSusChem, 2017, 10, 2660-2667.	6.8	84
48	SnO 2 nanowires decorated with forsythia-like TiO 2 for photoenergy conversion. Materials Letters, 2017, 202, 48-51.	2.6	6
49	Perovskite ink with wide processing window for scalable high-efficiency solar cells. Nature Energy, 2017, 2, .	39.5	499
50	Effect of Rubidium Incorporation on the Structural, Electrical, and Photovoltaic Properties of Methylammonium Lead lodide-Based Perovskite Solar Cells. ACS Applied Materials & Interfaces, 2017, 9, 41898-41905.	8.0	51
51	Acid Additives Enhancing the Conductivity of Spiroâ€OMeTAD Toward Highâ€Efficiency and Hysteresis‣ess Planar Perovskite Solar Cells. Advanced Energy Materials, 2017, 7, 1601451.	19.5	123
52	Facile fabrication of large-grain CH3NH3PbI3â^'xBrx films for high-efficiency solar cells via CH3NH3Br-selective Ostwald ripening. Nature Communications, 2016, 7, 12305.	12.8	444
53	Selective dissolution of halide perovskites as a step towards recycling solar cells. Nature Communications, 2016, 7, 11735.	12.8	129
54	Indium–Tin–Oxide Nanowire Array Based CdSe/CdS/TiO <sub>2</sub> One-Dimensional Heterojunction Photoelectrode for Enhanced Solar Hydrogen Production. ACS Sustainable Chemistry and Engineering, 2016, 4, 1161-1168.	6.7	33

#	Article	IF	CITATIONS
55	Facile fabrication of three-dimensional TiO 2 structures for highly efficient perovskite solar cells. Nano Energy, 2016, 22, 499-506.	16.0	40
56	Roughness of Ti Substrates for Control of the Preferred Orientation of TiO <sub>2</sub> Nanotube Arrays as a New Orientation Factor. Journal of Physical Chemistry C, 2015, 119, 13297-13305.	3.1	26
57	New Hybrid Hole Extraction Layer of Perovskite Solar Cells with a Planar p–i–n Geometry. Journal of Physical Chemistry C, 2015, 119, 27285-27290.	3.1	71
58	Green-emitting Lu <sub>3</sub> Al <sub>5</sub> O <sub>12</sub> :Ce <sup>3+</sup> phosphor as a visible light amplifier for dye-sensitized solar cells. RSC Advances, 2015, 5, 24737-24741.	3.6	19
59	Niobium Doping Effects on TiO <sub>2</sub> Mesoscopic Electron Transport Layerâ€Based Perovskite Solar Cells. ChemSusChem, 2015, 8, 2392-2398.	6.8	139
60	Epitaxial 1D electron transport layers for high-performance perovskite solar cells. Nanoscale, 2015, 7, 15284-15290.	5.6	49
61	Observation of anatase nanograins crystallizing from anodic amorphous TiO <sub>2</sub> nanotubes. CrystEngComm, 2015, 17, 7346-7353.	2.6	13
62	Nb-doped TiO <sub>2</sub> air-electrode for advanced Li-air batteries. Journal of Asian Ceramic Societies, 2015, 3, 77-81.	2.3	12
63	CdS-sensitized 1-D single-crystalline anatase TiO2 nanowire arrays for photoelectrochemical hydrogen production. International Journal of Hydrogen Energy, 2015, 40, 863-869.	7.1	18
64	Retarding charge recombination in perovskite solar cells using ultrathin MgO-coated TiO <sub>2</sub> nanoparticulate films. Journal of Materials Chemistry A, 2015, 3, 9160-9164.	10.3	167
65	Highly efficient and bending durable perovskite solar cells: toward a wearable power source. Energy and Environmental Science, 2015, 8, 916-921.	30.8	602
66	The effect of the number, position, and shape of methoxy groups in triphenylamine donors on the performance of dye-sensitized solar cells. Dyes and Pigments, 2015, 113, 390-401.	3.7	46
67	Electron emission of Au nanoparticles embedded in ZnO for highly conductive oxide. Applied Physics Letters, 2014, 104, .	3.3	11
68	Anionic Ligand Assisted Synthesis of 3-D Hollow TiO <sub>2</sub> Architecture with Enhanced Photoelectrochemical Performance. Langmuir, 2014, 30, 15531-15539.	3.5	10
69	A Hierarchically Organized Photoelectrode Architecture for Highly Efficient CdS/CdSe ensitized Solar Cells. Advanced Energy Materials, 2014, 4, 1300395.	19.5	10
70	Surface-area-tuned, quantum-dot-sensitized heterostructured nanoarchitectures for highly efficient photoelectrodes. Nano Research, 2014, 7, 144-153.	10.4	25
71	Controlled Interfacial Electron Dynamics in Highly Efficient Zn <sub>2</sub> SnO <sub>4</sub> â€Based Dye‣ensitized Solar Cells. ChemSusChem, 2014, 7, 501-509.	6.8	50
72	Transparent-conducting-oxide nanowire arrays for efficient photoelectrochemical energy conversion. Nanoscale, 2014, 6, 8649.	5.6	7

#	Article	IF	CITATIONS
73	Rheological and Electrochemical Properties of Nanoclay Added Electrolyte for Dye Sensitized Solar Cells. Electrochimica Acta, 2014, 144, 275-281.	5.2	6
74	Zn <sub>2</sub> SnO <sub>4</sub> -Based Photoelectrodes for Organolead Halide Perovskite Solar Cells. Journal of Physical Chemistry C, 2014, 118, 22991-22994.	3.1	92
75	1-D Structured Flexible Supercapacitor Electrodes with Prominent Electronic/Ionic Transport Capabilities. ACS Applied Materials & Interfaces, 2014, 6, 268-274.	8.0	34
76	A Simple Method To Control Morphology of Hydroxyapatite Nano- and Microcrystals by Altering Phase Transition Route. Crystal Growth and Design, 2013, 13, 3414-3418.	3.0	41
77	Anatase TiO2 nanorod-decoration for highly efficient photoenergy conversion. Nanoscale, 2013, 5, 11725.	5.6	44
78	Tailoring nanobranches in three-dimensional hierarchical rutile heterostructures: a case study of TiO2â€"SnO2. CrystEngComm, 2013, 15, 2939.	2.6	19
79	Controlled synthesis and Li-electroactivity of rutile TiO2 nanostructure with walnut-like morphology. Dalton Transactions, 2013, 42, 4278.	3.3	8
80	The effect of N-substitution and ethylthio substitution on the performance of phenothiazine donors in dye-sensitized solar cells. Dyes and Pigments, 2013, 97, 262-271.	3.7	45
81	BaSnO <sub>3</sub> Perovskite Nanoparticles for High Efficiency Dye‣ensitized Solar Cells. ChemSusChem, 2013, 6, 449-454.	6.8	78
82	TiO2 nanocrystals shell layer on highly conducting indium tin oxide nanowire for photovoltaic devices. Nanoscale, 2013, 5, 3520.	5.6	12
83	Î <sup>3</sup> -Al2O3 nanospheres-directed synthesis of monodispersed BaAl2O4:Eu2+ nanosphere phosphors. CrystEngComm, 2013, 15, 4797.	2.6	11
84	Surface Modified TiO2 Nanostructure with 3D Urchin-Like Morphology for Dye-Sensitized Solar Cell Application. Journal of Nanoscience and Nanotechnology, 2012, 12, 1305-1309.	0.9	4
85	Influence of Niobium Doping in Hierarchically Organized Titania Nanostructure on Performance of Dye-Sensitized Solar Cells. Journal of Nanoscience and Nanotechnology, 2012, 12, 5091-5095.	0.9	10
86	Aligned Photoelectrodes with Large Surface Area Prepared by Pulsed Laser Deposition. Journal of Physical Chemistry C, 2012, 116, 8102-8110.	3.1	29
87	Template-free synthesis of monodispersed Y3Al5O12:Ce3+ nanosphere phosphor. Journal of Materials Chemistry, 2012, 22, 12275.	6.7	17
88	Crystallographically preferred oriented TiO2 nanotube arrays for efficient photovoltaic energy conversion. Energy and Environmental Science, 2012, 5, 7989.	30.8	88
89	Synthesis and photovoltaic property of fine and uniform Zn <sub>2</sub> SnO <sub>4</sub> nanoparticles. Nanoscale, 2012, 4, 557-562.	5.6	71
90	Influence of Solvent and Bridge Structure in Alkylthio‣ubstituted Triphenylamine Dyes on the Photovoltaic Properties of Dye‣ensitized Solar Cells. Chemistry - an Asian Journal, 2012, 7, 1817-1826.	3.3	13

#	Article	IF	CITATIONS
91	Fabrication of TiO2/Tin-Doped Indium Oxide-Based Photoelectrode Coated with Overlayer Materials and Its Photoelectrochemical Behavior. Journal of Nanoscience and Nanotechnology, 2012, 12, 1390-1394.	0.9	4
92	Improved spectral response of sensitized photoelectrodes with the optical modulation layer. Electrochemistry Communications, 2012, 15, 29-33.	4.7	9
93	Facile hydrothermal synthesis of InVO4 microspheres and their visible-light photocatalytic activities. Materials Letters, 2012, 72, 98-100.	2.6	14
94	Transmittance optimized nb-doped TiO2/Sn-doped In2O3 multilayered photoelectrodes for dye-sensitized solar cells. Solar Energy Materials and Solar Cells, 2012, 96, 276-280.	6.2	35
95	Size-controlled synthesis of monodispersed mesoporous α-Alumina spheres by a template-free forced hydrolysis method. Dalton Transactions, 2011, 40, 6901.	3.3	35
96	Electronic Band Structure, Optical Properties, and Photocatalytic Hydrogen Production of Barium Niobium Phosphate Compounds (BaO–Nb <sub>2</sub> O <sub>5</sub> –P <sub>2</sub> O <sub>5</sub> ). European Journal of Inorganic Chemistry, 2011, 2011, 2206-2210.	2.0	7
97	Electronic band structures and photovoltaic properties of MWO4 (M=Zn, Mg, Ca, Sr) compounds. Journal of Solid State Chemistry, 2011, 184, 2103-2107.	2.9	68
98	Synthesis and Characteristics of Tb-Doped Y <sub>2</sub> SiO <sub>5</sub> Nanophosphors and Luminescent Layer for Enhanced Photovoltaic Cell Performance. Journal of Nanoscience and Nanotechnology, 2011, 11, 8748-8753.	0.9	13
99	Lowâ€Temperature Synthesis of Phaseâ€Pure 0D–1D BaTiO <sub>3</sub> Nanostructures Using H <sub>2</sub> Ti <sub>3</sub> O <sub>7</sub> Templates. European Journal of Inorganic Chemistry, 2010, 2010, 1343-1347.	2.0	13
100	Effects of crystal and electronic structures of ANb2O6 (A=Ca, Sr, Ba) metaniobate compounds on their photocatalytic H2 evolution from pure water. International Journal of Hydrogen Energy, 2010, 35, 12954-12960.	7.1	69
101	Two-Step Solâ^'Gel Method-Based TiO <sub>2</sub> Nanoparticles with Uniform Morphology and Size for Efficient Photo-Energy Conversion Devices. Chemistry of Materials, 2010, 22, 1958-1965.	6.7	166
102	A Newly Designed Nb-Doped TiO <sub>2</sub> /Al-Doped ZnO Transparent Conducting Oxide Multilayer for Electrochemical Photoenergy Conversion Devices. Journal of Physical Chemistry C, 2010, 114, 13867-13871.	3.1	30
103	Nb-Doped TiO <sub>2</sub> : A New Compact Layer Material for TiO <sub>2</sub> Dye-Sensitized Solar Cells. Journal of Physical Chemistry C, 2009, 113, 6878-6882.	3.1	210